Crosstalk and SNR Measurements using a Multi-Antenna RFID Reader with Active Carrier Compensation

*Robert Langwieser *, Christoph Angerer *, Arpad L. Scholtz, and Markus Rupp*
*Christian Doppler Laboratory for Wireless Technologies for Sustainable Mobility **
Institute of Communications and Radio-Frequency Engineering
Vienna University of Technology, Austria
{rlang, cangerer, ascholtz, mrupp}@nt.tuwien.ac.at

***Abstract* - In this paper we show the dependence of the Signal to Self Interference Ratio (SSIR) and of the Signal to Noise Ratio (SNR) on the transmit power level of the reader and the transponder position. We describe the conducted measurements with our multi-antenna Radio Frequency Identification (RFID) research and development environment and compare passive transmitter-receiver isolation due to spatially separated antennas with additional active crosstalk compensation. With the active compensation we have achieved an SSIR improvement of more than 55 dB. In scenarios with active carrier compensation the evaluation of the interference to noise ratio at the receivers at different transponder positions shows that the compensated crosstalk is at least composed of two different parts. One part is the direct crosstalk from the reader transmitter antenna to the receiver antennas and a second part of the interference is reflected by the transponder and superposed at the receive antennas.**

I. Introduction

In the Ultra High Frequency (UHF) domain communication of passive or semi-active Radio Frequency Identification (RFID) systems is based on the technique of backscatter modulation [1]. This means that a part of a transmitted Continuous Wave (CW) Radio Frequency (RF) signal is reflected by a target to a receiver. In RFID systems transmitter and receiver are combined into one device called interrogator or reader and the backscattering device is called transponder or tag. The backscattering requires that the transmitter and the receiver of the reader operate at the same frequency at the same time. Therefore, the transmitter can not be switched off during reception. Furthermore, the transmit signal and the receive signal can not be separated by conventional filtering. This leads to a strong self interference at the receiver during the whole communication process. In the case of passive RFID the transponders are additionally powered by the CW signal of the reader.

The ratio of the received transponder response to the self interference, Signal to Self Interference Ratio (SSIR), can be -60 dB [2] and worse depending on the antenna configuration and the distance of the transponder. To reduce the linearity requirements of the receiver and to avoid large DC offsets at the receiver the isolation between transmitter and receiver has to be improved either with passive or active techniques [3]- [8]. In this contribution we discuss the system performance utilizing an experimental multi-antenna reader and increased isolation based on separated transmit and receive antennas and furthermore with active carrier compensation based on vector modulators [9]. The approach of two receivers allows to measure at two spatial separated receive positions at the same time. Moreover, multi-antenna scenarios like beam forming or diversity techniques are discussed for RFID [10], [11]. Furthermore we look into the influence of the transmit power level onto the SSIR and the Signal to Noise Ratio (SNR).

In Section II. we describe our measurement environment and the measurement procedure and in Section III. we present and discuss our results. Finally, in Section IV. we conclude our paper.

II. Measurement Environment

We performed the measurements presented in this paper with our multi-antenna RFID research environment [12] [13]. This environment allows for a very flexible reader configuration with up to two transmitters and two receivers. The experimental reader can be divided into three building blocks: the digital baseband [14], the RF frontends, and the antennas. A system overview is illustrated in Figure 1. The protocol issues were processed in a DSP of the digital

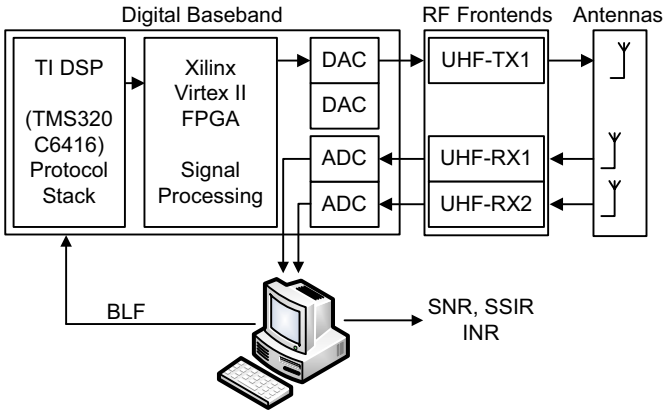

Figure 1 - Measurement setup overview

baseband unit and the transmit sequence for powering the transponder and to communicate with the transponder is generated by a Field Programable Gate Array (FPGA). Via a Digital-to-Analog Converter (DAC) the analog UHF-transmitter is connected. Finally, the antennas are placed in a separate room and are connected with cables to the transmitter and the receivers. Two analog UHF-receivers are connected to the two Analog-to-Digital Converters (ADCs) of the digital baseband. The samples are directly transferred and stored to a personal computer (PC). The data processing is performed later on off-line in Matlab.

We have measured in the UHF band at a frequency of 866 MHz with a commercially available passive transponder for all conducted measurements. In Figure 2 the RF frontend configuration with crosstalk compensation is illustrated. Transmitter and receivers perform as linear frequency transponders. This transponders are connected to the digital baseband at 13.33 MHz and perform the frequency up-conversion to the desired UHF band or the down-conversion respectively. At the UHF-transmitter the output power level can be adjusted continuously over a range of 55 dB. Additionally, two crosstalk or Carrier Compensation Units (CCU1 and CCU2) are part of the frontend setup. A fraction of the transmit signal is distributed to the two vector modulators of the CCUs. The outputs of the CCUs are added via the directional couplers into the receivers RX1 and RX2 and used to compensate the crosstalk from antenna TXA1 to the antennas RXA1 and RXA2 at the receivers. The two vector modulators allow to adjust separately the compensation signals for the two receivers. For perfect

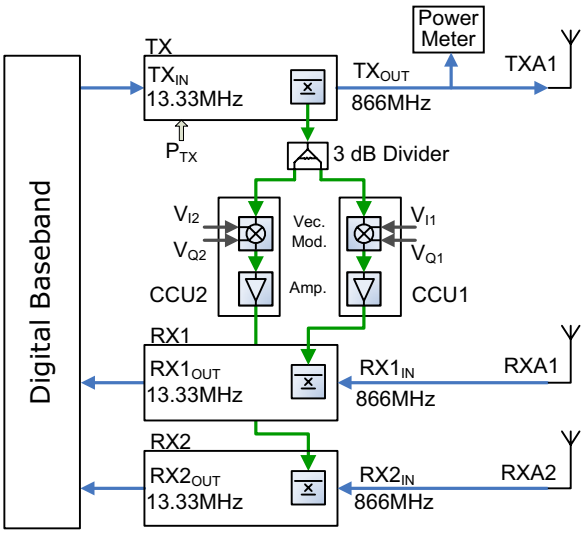

FIGURE 2 - RF FRONTEND MEASUREMENT CONFIGURATION

compensation the compensation signals should have the same magnitude as the crosstalk signals and a 180° phase shift to them at the receiver. The CCUs can be adjusted separately via the control voltages V_{I1} and V_{Q1} and V_{I2} and V_{Q2} respectively. The amplitude adjustment range is 50 dB and the phase can be adjusted in a full 360° range. For all measurements presented in this paper the CCUs were adjusted manually. For the measurements without compensation the CCUs are disconnected from the receivers.

Finally, Figure 3 shows the configuration of the reader antennas and the transponder. As mentioned before, the antennas and the

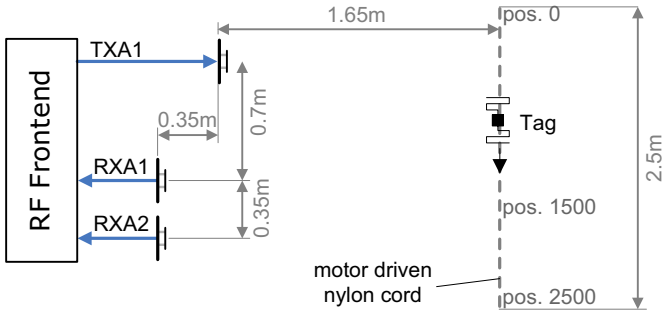

FIGURE 3 - ANTENNA CONFIGURATION

transponder are placed in a separate measurement room. All measurements were conducted in a static low-fading environment with direct line of sight between reader antennas and transponder. The reader antennas are right hand circularly polarized patch antennas. The transmit antenna TXA1 has a gain of 9 dBi and the gain of the receive antennas RXA1 and RXA2 is 8 dBi. The positions of the antennas were chosen for a good decoupling of around 40 dB between the transmitter and receiver one and 43 dB between the transmitter and receiver two.

We employed a commercially available EPCglobal class 2 standard [15] compliant transponder, mounted on a motor driven nylon cord. Moving this cord the position of the transponder was changed automatically from the outer left position pos. 0000 in steps of 100 mm to pos. 2500 during the measurements. At each position 25 QUERY commands were transmitted and the responding 16 bit random numbers from the transponder were recorded for both receivers. Between two communication cycles the CW signal of the reader is switched off to reset the transponder.

III. MEASUREMENT RESULTS

Two different measurement scenarios were conducted: The first scenario is without an active compensation and the second scenario has the active compensation in addition to the spatial isolation. Furthermore, all measurements were performed at three different transmit power levels and at a Backscatter Link Frequency (BLF) of the transponder of 320 kHz.

3.1 Spatial isolation without active compensation

In this scenario the isolation of the transmit antennas is only due to their spatial configuration shown in Figure 3. In Figure 4 the results for the SNR in terms of E_b/N_0 are presented for different transmit power levels and a BLF of 320 kHz. First of all, the two receive paths for

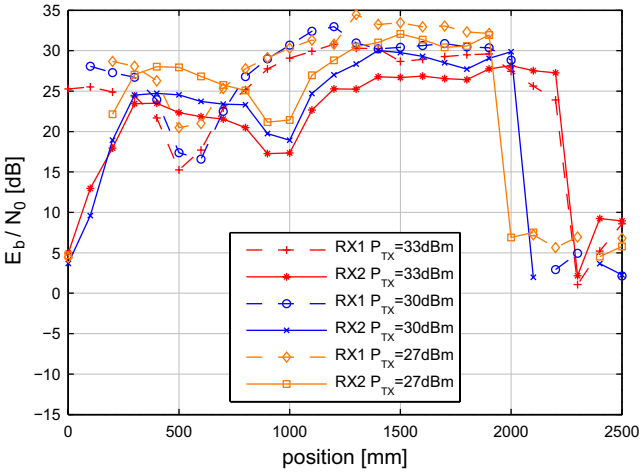

FIGURE 4 - SIGNAL TO NOISE RATIO WITHOUT CCUS FOR DIFFERENT TRANSMIT POWER LEVELS

receiver RX1 and RX2 show comparable behavior. The spatial shift of the results of the two receivers in the figure is due to the distance between their two antennas. Furthermore, we can observe a variation of the SNR depending on the transponder position which is caused on the one hand due to the radiation pattern of the antennas and on the other hand due to multi path propagation in the measurement room. At a transmit power of 33 dBm we observe at the outer left positions, from pos. 0000 to pos. 0300, that only antenna one (RXA1) shows sufficient SNR for decoding the transponder response. This indicates clearly that spatial diversity can improve the overall system performance. Observing only the receive signal at receiver two could further lead to a misinterpretation of the situation that the transponder is not sufficiently powered by the reader. This situation can be seen at the outer right positions from pos. 2100 to pos. 2500. Here both receivers cannot receive a transponder response.

Furthermore, we can observe in this figure that the SNR of the received backscatter signal is improved by decreasing the transmit power. This also reduces the leaking noise from the transmitter into the receiver while the received signal stays more or less constant. Additionally, the reduction of the transmit power reduces the energy transfer to the transponder and therefore the transponder is not responding at lower transmit power (-27 dBm) at the outer left positions from pos. 0000 to pos. 0200.

In Figure 5 the results for the signal to self interference are presented of the same measurements. Similar observations can be done for the SSIR graph than for the SNR graph. The SSIR varies from -75 dB for a weak response at highest transmit power (33 dBm) at antenna two at position pos. 0000 and -31 dB for the lowest transmit power of 27 dBm at transponder position somewhere between the transmit and receive antennas. Comparable to the SNR results the SSIR is improved for decreased transmit power level due to the concurrent reduction of crosstalk level at the reader. Finally, Figure 6

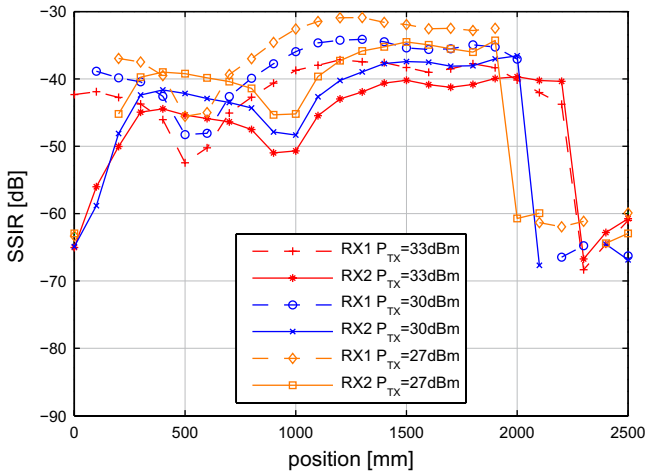

FIGURE 5 - SIGNAL TO SELF INTERFERENCE RATIO WITHOUT CCUS FOR DIFFERENT TRANSMIT POWER LEVELS

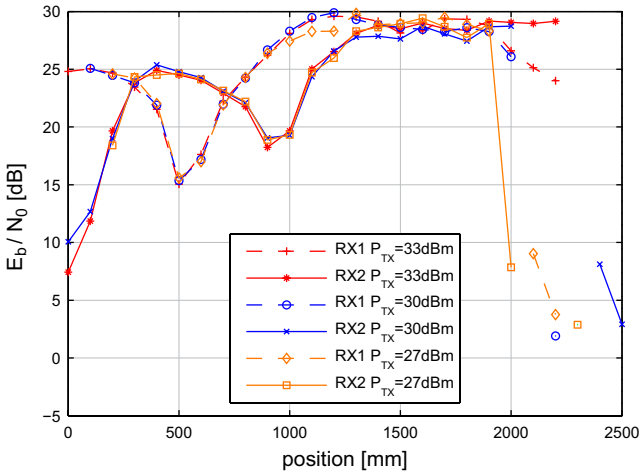

FIGURE 7 - SIGNAL TO NOISE RATIO EVALUATION WITH CCU FOR DIFFERENT TRANSMIT POWER LEVELS

shows the Interference to Noise Ratio (INR) of this measurements for the three different transmit power levels. This measure is based on the

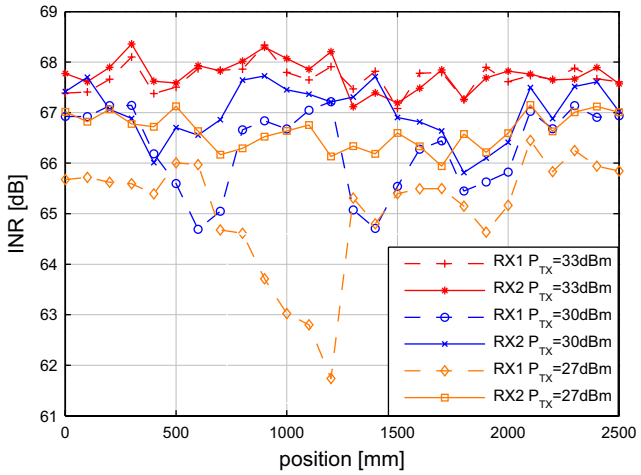

FIGURE 6 - INTERFERENCE TO NOISE RATIO WITHOUT ACTIVE COMPENSATION FOR DIFFERENT TRANSMIT POWER LEVELS.

observation that the noise level is constant and independent from the transponder position for constant transmit power levels. We thus have a measure which only shows us the dependence of the interference without the requirement of a transponder response. For this scenario the INR shows only small variations due to changes of the transponder position.

3.2 Active carrier compensation

For this scenario the antenna configuration is unchanged but in addition the CCUs were connected to the receivers and manually adjusted at position pos. 1500 for best carrier compensation. The measurements before are now used as references for comparison. Figure 7 shows the signal to noise ration for the two receivers with the CCUs in operation. The overall behavior of the variation of the SNR depending on the transponder position is very similar compared to the measurements without active compensation. Nevertheless, the improvement in SNR due to reduced transmit power can not be observed as before. The overall SNR performance of all measurements is now reduced to comparable values of the reference measurement with the highest transmit power level. This decreased SNR performance is due to the additional noise injection caused by the CCUs.

Figure 8 shows the performance of the active carrier compensation direct in terms of SSIR. At the highest transmit power level of 33 dBm

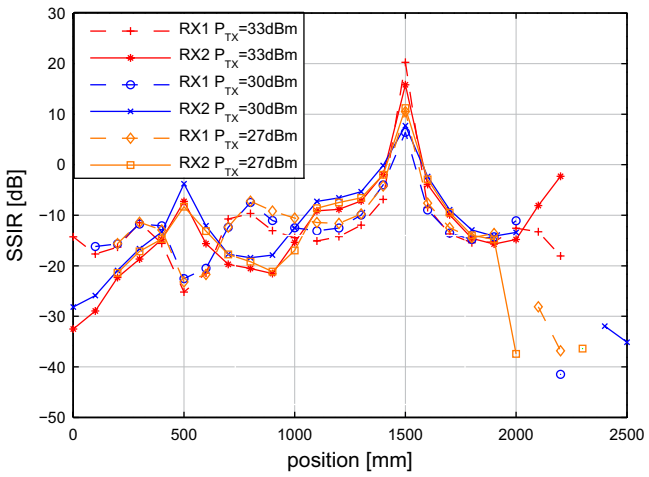

FIGURE 8 - SIGNAL TO SELF INTERFERENCE EVALUATION WITH CCUS FOR DIFFERENT TRANSMIT POWER LEVELS

the additional improvement with active carrier compensation is more than 55 dB at pos. 1500 at which the CCUs were adjusted. Also at all other transponder positions a minimum improvement of more than 20 dB can be observed. Furthermore, at dedicated positions the SSIR improvement starts to increase again.

Finally, Figure 9 shows the interference to noise ration of the two receivers with the CCUs in operation. Here also the noise floor is constant and transponder position independent. The observed variations are only due to the interference part. The increase and decrease of the interference shows that the interference is not only direct from antenna TX1 to the receive antennas RX1 and RX2. Additionally to the direct crosstalk path also a part of the radiated carrier is reflected by the transponder. At pos. 1500 both parts are compensated by the CCUs. Due to the movement of the transponder this indirect part changes in magnitude and phase. At dedicated positions the phase shift compared to the compensation signal is 360°, at these positions we have a maximum in the INR, or the phase shift is 180°, at these positions we have a local minimum in the INR.

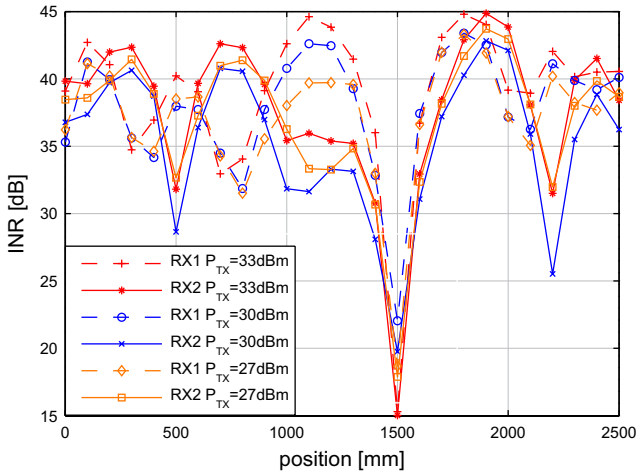

FIGURE 9 - INTERFERENCE TO NOISE RATIO EVALUATION WITH CCU FOR DIFFERENT TRANSMIT POWER LEVELS

IV. CONCLUSION

In this paper we presented measurements with our multi-antenna RFID research and development environment at different transmit power levels with and without the use of active carrier compensation at the reader's receivers. We described the measurement setup with one transmitter and two receivers at the reader and a remotely controlled moveable commercially available transponder. We showed the transmit power dependence of the receive parameters SNR, and SSIR in the scenario without active compensation. The measurements with two receivers show that we have to distinguish between to different cases if we do not receive a response. The first case is that the transponder does not receive sufficient energy by the reader and is not responding. In the second case the transponder response cannot be observed by the receiver due to destructive interference at the receiver antenna in a multi path environment. Operating with just on single receive antenna does not allow to distinguish.

Furthermore we showed an SSIR improvement of more than 55 dB in the scenario were the active compensation is applied. Moreover the evaluation of the interference to noise ratio at the receivers shows directly that also a part of the interference or carrier signal is reflected by the transponder. The phase of this interference part change along the different positions of the transponder and fulfills periodically the required 180° phase relationship at the receivers for the active compensation.

ACKNOWLEDGEMENTS

The financial support by the Federal Ministry of Economy, Family and Youth and the National Foundation for Research, Technology and Development is gratefully acknowledged. Furthermore, we would like to thank our industrial partner Infineon Technologies for enabling this work and supporting us with many advices and discussions. In addition, we would like to thank Austrian Institute of Technology (previous Austrian Research Centers), who supported us with the SmartSim rapid prototyping board.

REFERENCES

[1] H. Stockman. Communication by means of reflected power. *Proceedings of the IRE*, 36(10):1196–1204, Oct. 1948.

[2] J.-P. Curty, M. Declercq, C. Dehollain, and N. Joehl. *Design and Optimization of Passive UHF RFID Systems.* Springer, New York, 2007.

[3] K. Penttilä, L. Sydänheimo, and M. Kivikoski. Implementation of Tx/Rx isolation in an RFID reader. In *Int. J.Radio Frequency Identification Technology and Applications 2008 - Book of Proceedings*, pages 74–89, 2006.

[4] L. W. Mayer, R. Langwieser, and A. L. Scholtz. Evaluation of passive carrier-suppression techniques for UHF RFID systems. In *2009 IEEE MTT-S International Microwave Workshop on Wireless Sensing, Local Positioning and RFID*, Cavtat, Croatia, September 2009.

[5] J. Y. WANG, W. Z. Cui, W. Ma, J. T. Huangfu, and L. X. Ran. Isolation enhancement based on adaptive leaking cancellation. In *Progress In Electromatics Research Symposium*, pages 1059–1063, Xián, China, March 2010.

[6] A. Sadeghfam and H. Heuermann. Electrically tunable bandpass filter with integrated carrier suppression for UHF RFID systems. In *European Conference on Wireless Technology, 2008. EuWiT 2008.*, pages 306–309, Oct. 2008.

[7] Jeiyoung Lee, Jaehong Choi, Kang Ho Lee, Bonkee Kim, Minsu Jeong, Youngho Cho, Heeyong Yoo, Kyoungon Yang, S. Kim, Seong-Mo Moon, Jae-Young Lee, Sangkyu Park, Wanchul Kong, Jin Kim, Tae-Ju Lee, Bo-Eun Kim, and Beom-Kyu Ko. A uhf mobile rfid reader ic with self-leakage canceller. In *2007 IEEE Radio Frequency Integrated Circuits (RFIC) Symposium*, pages 273 –276, 3-5 2007.

[8] G. Lasser, R. Langwieser, and A. L. Scholtz. Broadband suppression properties of active leaking carrier cancellers. In *IEEE RFID 2009, 2009 IEEE International Conference on RFID*, Orlando, USA, April 2009.

[9] P. D. L. Beasley, A. G. Stove, B. J. Reits, and B.-O. As. Solving the problems of a single antenna frequency modulated CW radar. In *Record of the IEEE 1990 International Radar Conference*, pages 391–395, 1990.

[10] C. Angerer, R. Langwieser, G. Maier, and M. Rupp. Maximal ratio combining receivers for dual antenna RFID readers. In *2009 IEEE MTT-S International Microwave Workshop Series on Wireless Sensing, Local Positioning, and RFID*, pages 21–24, Cavtat, Croatia, September 2009.

[11] M. F. Demirkol M. A. Ingram and D. Kim. Transmit diversity and spatial multiplexing for RF links using modulated backscatter. In *International Symposium on Signals, Systems, and Electronics (ISSSE01)*, Tokyo, Japan, Juli 2001.

[12] C. Angerer, M. Holzer, B. Knerr, and M. Rupp. A flexible dual frequency testbed for RFID. In *TridentCom '08: Proceedings of the 4th International Conference on Testbeds and Research Infrastructures for the Development of Networks & Communities*, Innsbruck, Austria, 2008.

[13] R. Langwieser, C. Angerer, and A. L. Scholtz. A UHF frontend for MIMO applications in RFID. In *2010 IEEE Radio and Wireless Symposium*, New Orleans, USA, January 2010.

[14] G. Meindl, R. Kloibhofer, F. Kaltenberger, and G. Humer. Multi-standard development and measuring platform for MIMO-sofware definded radio. In *13th European Signal Processing Conference (EUSIPCO)*, Antalya, Turkey, September 2005.

[15] EPCGlobal. EPC radio-frequency identity protocols class-1 generation-2 UHF RFID. `http://www.epcglobalinc.org`.